

# The critical role of atypical protein kinase C in activating hepatic SREBP-1c and NFκB in obesity

Mini P. Sajan,<sup>\*\*\*</sup> Mary L. Standaert,<sup>\*</sup> Sonali Nimal,<sup>†</sup> Usha Varanasi,<sup>†</sup> Tina Pastoor,<sup>†</sup> Stephen Mastorides,<sup>\*</sup> Ursula Braun,<sup>\*\*</sup> Michael Leitges,<sup>§</sup> and Robert V. Farese<sup>1,\*,†,\*\*,§</sup>

James A. Haley Veterans Hospital,<sup>\*</sup> Tampa, FL; Roskamp Institute,<sup>†</sup> Sarasota, FL; Biotechnology Centre of Oslo,<sup>§</sup> Oslo, Norway; and College of Medicine,<sup>\*\*</sup> University of South Florida, Tampa, FL

**Abstract** Obesity is frequently associated with systemic insulin resistance, glucose intolerance, and hyperlipidemia. Impaired insulin action in muscle and paradoxical diet/insulin-dependent overproduction of hepatic lipids are important components of obesity, but their pathogenesis and inter-relationships between muscle and liver are uncertain. We studied two murine obesity models, moderate high-fat-feeding and heterozygous muscle-specific PKC-λ knockout, in both of which insulin activation of atypical protein kinase C (aPKC) is impaired in muscle, but conserved in liver. In both models, activation of hepatic sterol receptor element binding protein-1c (SREBP-1c) and NFκB (nuclear factor-kappa B), major regulators of hepatic lipid synthesis and systemic insulin resistance, was chronically increased in the fed state. In support of a critical mediatory role of aPKC, in both models, inhibition of hepatic aPKC by adenovirally mediated expression of kinase-inactive aPKC markedly diminished diet/insulin-dependent activation of hepatic SREBP-1c and NFκB, and concomitantly improved hepatosteatosis, hypertriglyceridemia, hyperinsulinemia, and hyperglycemia. Moreover, in high-fat-fed mice, impaired insulin signaling to IRS-1-dependent phosphatidylinositol 3-kinase, PKB/Akt and aPKC in muscle and hyperinsulinemia were largely reversed. In obesity, conserved hepatic aPKC-dependent activation of SREBP-1c and NFκB contributes importantly to the development of hepatic lipogenesis, hyperlipidemia, and systemic insulin resistance. Accordingly, hepatic aPKC is a potential target for treating obesity-associated abnormalities.—Sajan, M. P., M. L. Standaert, S. Nimal, U. Varanasi, T. Pastoor, S. Mastorides, U. Braun, M. Leitges, and R. V. Farese. **The critical role of atypical protein kinase C in activating hepatic SREBP-1c and NFκB in obesity.** *J. Lipid Res.* 2009. 50: 1133–1145.

**Supplementary key words** atypical protein kinase C • high fat feeding • hyperlipidemia • insulin • insulin resistance • IRS-1 • IRS-2 • liver • muscle • NFκB • obesity • phosphatidylinositol 3-kinase • SREBP-1c • type 2 diabetes

Obesity, particularly when accompanied by systemic insulin resistance, glucose intolerance, and hyperlipidemia (i.e., a “metabolic syndrome”) is a global health problem and a frequent forerunner of type 2 diabetes mellitus. Whereas both exogenous/diet-induced and genetically determined obesity can produce insulin resistance and metabolic syndrome features, vice versa, systemic insulin resistance can produce obesity and metabolic syndrome features. However, mechanisms underlying lipid abnormalities and insulin resistance in these situations, and the critical interplay between muscle and liver, are poorly understood.

The high-fat–fed (HFF) mouse model is useful for studying diet-induced obesity-related insulin resistance. In our experience, feeding mice a Western-type 20% milk high-fat diet for 3–4 weeks leads to diminished insulin activation of phosphatidylinositol (PI) 3-kinase (PI3K) effectors, atypical protein kinase C (aPKC) and protein kinase B (PKB/Akt) in muscle (1, 2), with little or no effect on hepatic aPKC and PKB/Akt activation (1). In this HFF model, we have observed no increases in basal (unstimulated) activities of conventional (α,β2) or novel (δ,ε) PKCs in liver, despite observing increases in muscle (unpublished). Accordingly, our HFF model may partly differ from others wherein higher dietary fat was used, thereby activating hepatic novel PKCs.

Insulin signaling to aPKC and PKB/Akt (particularly the PKBβ/Akt2 isoform) is important, as these kinases control key metabolic processes, viz., glucose transport in muscle is controlled by both aPKC and PKB/Akt, enzymes regulating hepatic glucose output are mainly controlled by PKB/Akt (3, 4), and hepatic sterol receptor element binding protein-1c (SREBP-1c), which trans-activates multiple genes involved in lipid synthesis, can be controlled by both aPKC (3, 4) and PKB/Akt (5, 6). Also, hepatic NFκB (nuclear

*This work was supported by funds from the Department of Veterans Affairs Merit Review Program and the National Institutes of Health DK-38079 (R. V. F.), and by the Deutsche Forschungsgemeinschaft Sta314/2-1 and KE246/7-2 (M. L.).*

*Manuscript received 8 October 2008 and in revised form 16 January 2009.*

*Published, JLR Papers in Press, February 6, 2009.  
DOI 10.1194/jlr.M800520-JLR200*

Abbreviations: aPKC, atypical protein kinase C; SREBP-1c, hepatic sterol receptor element binding protein-1c; KO, knockout; NFκB, nuclear factor-kappa B.

<sup>1</sup>To whom correspondence should be addressed.

e-mail: rfarese@health.usf.edu

factor-kappa B), which is activated in HFF mice and linked to systemic insulin resistance (7, 8) and inflammation, can be activated by aPKC through (a) phosphorylation/activation of I $\kappa$ B kinase (IKK $\beta$ ), which phosphorylates I $\kappa$ B $\beta$ , thereby releasing NF $\kappa$ B for translocation to nuclear transcription sites (9); and (b) phosphorylation/activation of the p65/RelA subunit of NF $\kappa$ B (10). However, insulin effects on IKK $\beta$  and NF $\kappa$ B are unknown.

Differences in activation of aPKC and PKB/Akt in muscle and liver in HFF mice most likely reflect tissue-specific variations in PI3K activation by insulin receptor substrates (IRS), IRS-1 and IRS-2. However, definitive information on PI3K activation in HFF mice is lacking, and findings in other HFF models are inconsistent. In rats fed 58% lard, activation of hepatic IRS-1- and IRS-2-dependent PI3K is oddly enough enhanced (11); in rats fed 21% milk fat, activation of muscle aPKC by insulin *in vivo* and PI-3,4,5-(PO $_4$ ) $_3$  (PIP $_3$ ) *in vitro* is impaired, but activation of IRS-1- and IRS-2-dependent PI3K is intact (12); in rats fed 65% fat, aPKC and PKB activation in muscle is diminished (13).

Germane to tissue-specific differences in aPKC/PKB activation, findings from knockout mice suggest that IRS-1 and IRS-2 activate separate PI3K pools that couple differently to these downstream effectors during insulin action, depending upon the tissue. Thus, in IRS-1 knockout mice, insulin activation of both PKB/Akt (14, 15) and aPKC (15) is impaired in muscle, whereas in liver, PKB/Akt activation is impaired (14, 15), but aPKC activation is conserved (15). In IRS-2-deficient hepatocytes, activation of aPKC, as well as PKB/Akt, is impaired (16). To summarize, IRS-1 controls both aPKC and PKB/Akt in muscle, whereas in liver, IRS-2 controls aPKC, and both IRS-1 and IRS-2 control PKB/Akt activation by insulin.

In HFF mice, we found that inhibition of hepatic aPKC by adenovirally mediated expression of kinase-inactive (KI) aPKC largely reversed excessive increases in hepatic SREBP-1c and IKK $\beta$ /NF $\kappa$ B activities, thereby improving downstream targets of SREBP-1c and NF $\kappa$ B, hyperlipidemia, insulin signaling in muscle, hyperinsulinemia, and hyperglycemia. Similarly, in a genetic obesity model, heterozygous muscle-specific knockout of PKC- $\lambda$  (M $\lambda$ -Het-KO) mice [wherein (a) aPKC activation is selectively impaired in muscle, thereby compromising insulin-stimulated glucose transport, (b) insulin signaling and actions in liver and adipocytes are intact, and (c) feeding- and insulin-dependent activation of hepatic SREBP-1c and IKK $\beta$ /NF $\kappa$ B are excessive, thereby producing abdominal obesity, hepatosteatosis, hyperlipidemia, and glucose intolerance (17)], we observed comparable dependency of hepatic SREBP-1c and IKK $\beta$ /NF $\kappa$ B on hepatic aPKC and, moreover, similar phenotypic improvements following administration of adenovirus expressing KI-aPKC.

## EXPERIMENTAL PROCEDURES

### Experimental mice

In HFF studies, male C57Bl/6 mice, 8–12 weeks of age, were obtained from Harlan Industries, housed in a temperature-

controlled environment with alternating 12-h light and dark cycles, and fed ad lib with either a standard low-fat laboratory chow diet [Harlan Teklad 20/18 with 5% fat (i.e., 10% of calories)] or a moderately high-fat Western-type diet [Harlan Teklad T01064 with 20% by weight anhydrous milk fat and 1% corn oil (i.e., 42% of calories with fatty acid composition in g fatty acid-length: unsaturation/kg diet as follows: butyric-4:0, 7.6; caproic-6:0, 4.6; caprylic-8:0, 2.2; capric-10:0, 4; capric-11:0, 0.2; lauric-12:0, 6.2; myristic-14:0, 23.4; myristic-14:1, 1.6; myristic-15:0, 3.2; palmitic-16:0, 53.6; palmitoleic-16:1, 3.8; margaric-17:0, 1.4; margaric-17:1, 0.4; stearic-18:0, 25.2; oleic-18:1, 59.15; linoleic-18:2, 11.5; linolenic-18:3, 1.1; linolenic-20:1, 0.4; arachidonic-20:4, 0.2)] for 3–4 weeks prior to experimental use. In some cases, where indicated as “fasted,” food (but not water) was withheld overnight for approximately 16–20 h before killing.

Wild-type and heterozygous muscle-specific PKC- $\lambda$  knockout (M $\lambda$ -Het-KO) were generated as described (17).

All experimental procedures were approved by the James A. Haley Veterans Administration Medical Center Research and Development Committee; Institutional Animal Care and Use Committees of the University of South Florida College of Medicine; and the Roskamp Research Institute.

### In vivo insulin treatments

Where indicated, mice were injected intraperitoneally (IP) 5 min before killing, or intramuscularly (IM) 15 min before killing, with either physiological (0.9%) saline or saline containing 1U insulin/kg body weight. IRS-1/2-dependent PI3K activation in liver is maximal at 2–5 min after IP insulin treatment, but 15 min is optimal for studies of insulin stimulation of IRS-1/2-dependent PI3K in muscle and for aPKCs and PKB/Akt in both muscle and liver (1, 2, 12, 15, 17–23).

### Tissue and immunoprecipitate preparations

As described (1, 2, 12, 15, 17–23), vastus lateralis muscles and liver were rapidly removed and homogenized (Polytron) in ice-cold buffer containing 0.25 M sucrose, 20 mM Tris/HCl (pH 7.5), 2 mM EGTA, 2 mM EDTA, 1 mM phenylmethylsulfonyl fluoride (PMSF), 20  $\mu$ g/ml leupeptin, 10  $\mu$ g/ml aprotinin, 2 mM Na $_4$ P $_2$ O $_7$ , 2 mM Na $_3$ VO $_4$ , 2 mM NaF, and 1  $\mu$ M microcystin. After centrifugation for 10 min at 700 *g* to remove unbroken cells, debris, nuclei, and floating fat, the resulting cell lysates were stored at  $-70^\circ\text{C}$ . After addition of 1% TritonX-100, 0.6% Nonidet, and 150 mM NaCl, lysates were cleared of insoluble materials by low-speed centrifugation and subsequently immunoprecipitated with antibodies that target (a) aPKCs (rabbit polyclonal antiserum from Santa Cruz Biotechnologies; recognizes C termini of both PKC- $\lambda$  and PKC- $\zeta$ ); (b) PKB/Akt; and (c) IRS-1 or IRS-2 (rabbit polyclonal antisera from Upstate Cell Signaling, Inc.). Immunoprecipitates were collected on Sepharose-AG beads (Santa Cruz Biotechnologies) and activities of aPKC, PKB, and PI3K were assayed as described below.

### aPKC activity assay

aPKC activity was measured as described (1, 2, 12, 15, 17–23). Briefly, aPKCs were immunoprecipitated from lysates with a rabbit polyclonal antiserum (Santa Cruz Biotechnologies) that recognizes C termini of both PKC- $\zeta$  and PKC- $\lambda$  [whereas mouse muscle contains mainly PKC- $\lambda$  and little PKC- $\zeta$  (22), mouse liver contains substantial amounts of both PKC- $\zeta$  and PKC- $\lambda$  (11)], collected on Sepharose-AG beads (Santa Cruz Biotechnologies), and incubated for 8 min at 30 $^\circ\text{C}$  in 100  $\mu$ l buffer containing 50 mM Tris/HCl (pH,7.5), 100  $\mu$ M Na $_3$ VO $_4$ , 100  $\mu$ M Na $_4$ P $_2$ O $_7$ , 1 mM NaF, 100  $\mu$ M PMSF, 4  $\mu$ g phosphatidylserine (Sigma), 50  $\mu$ M [ $\gamma$ - $^{32}\text{P}$ ]ATP (NEN Life Science Products), 5 mM MgCl $_2$ , and, as substrate, 40  $\mu$ M serine analog of the PKC- $\epsilon$  pseudosubstrate (BioSource).

In some cases, assays were conducted in the presence of 10  $\mu$ M PIP<sub>3</sub>, which maximally (like exogenous insulin treatment) activates aPKCs immunoprecipitated from muscles of control noninsulin-treated rodents (12, 17). After incubation, <sup>32</sup>P-labeled substrate was trapped on P-81 filter papers and counted.

### PKB/Akt activation

Total PKB $\alpha$ / $\beta$  (Akt1/2) enzyme activity was measured using a kit obtained from Upstate Cell Signaling, as described (1, 2, 12, 15, 17–23). In brief, PKB/Akt was immunoprecipitated from lysates with rabbit polyclonal antibodies, collected on Sepharose-AG beads, and incubated as per kit directions. Total PKB/Akt activation was also assessed by immunoblotting for phosphorylation of serine-473.

### PI3K activation

IRS-1–dependent and IRS-2–dependent PI3K activities were determined as described (1, 2, 12, 15, 17–23). In brief, IRS-1 and IRS-2 immunoprecipitates were incubated with PI and examined for incorporation of <sup>32</sup>PO<sub>4</sub> into PI-3-PO<sub>4</sub>, which was purified by thin layer chromatography and quantified with a BioRad Molecular Analyst Phosphor-Imager system.

### Western analyses

Western analyses were conducted as described (1, 2, 12, 15, 17–23) using the following antibodies and antisera for immunodetection after resolution of lysate proteins on SDS-PAGE: (a) rabbit polyclonal anti-PKC- $\zeta$ / $\lambda$  antiserum (Santa Cruz Biotechnologies); (b) rabbit polyclonal anti-PKB antiserum (Upstate Cell Signaling); (c) rabbit polyclonal anti-phospho-serine-473-PKB antiserum (New England BioLabs); (d) rabbit polyclonal anti-IRS-1 antiserum (Upstate Cell Signaling); (e) rabbit polyclonal anti-IRS-2 antiserum (Upstate Cell Signaling); (f) rabbit polyclonal anti-p85/PI3K antiserum (Upstate Cell Signaling); (g) rabbit polyclonal anti-thr-410-PKC- $\zeta$  (or thr-411-PKC- $\lambda$ ) antiserum (Upstate Cell Signaling); (h) rabbit polyclonal anti-SREBP-1 (Neomarkers, Inc.); and anti-p65/RelA subunit of NF $\kappa$ B (Santa Cruz Biotechnologies).

### Glucose uptake into skeletal muscle in vivo

Glucose uptake was determined as described (12, 17, 20, 21). Briefly, mice were injected IP with 0.9% saline containing tracer amounts of [<sup>3</sup>H]2-deoxyglucose (transported and phosphorylated but not metabolized hexose) and [<sup>14</sup>C]L-glucose (a non-transported hexose used to correct for nonspecific trapping of extra-cellular fluid in muscle), and where indicated, insulin (1U/kg). 10 min later, muscle samples and serum were obtained. Total hexose (largely glucose) uptake was calculated from the specific activity of serum hexose (i.e., [<sup>3</sup>H]2-deoxyglucose radioactivity divided by serum glucose level) and muscle uptake of [<sup>3</sup>H]2-deoxyglucose.

### Adenoviral studies

Adenoviruses were propagated in HEK-293 cells, purified by cesium chloride centrifugation and dialyzed against Krebs Ringer phosphate buffer. Adenovirus vector or adenovirus encoding KI-PKC- $\zeta$  [ $2.5 \times 10^{12}$  plaque-forming units (PFU)/kg body weight] was administered intravenously (IV; tail vein) to HFF mice or M $\lambda$ -Het-KO mice. After 4 days, mice were subjected to overnight fasting or continued feeding of their usual diet for 24 h, as indicated. On the fifth day, where indicated, mice were injected IM with saline or insulin in saline, and 15 min later, mice were killed and liver and muscle samples were obtained. Note

that (a) adenoviral treatments did not increase serum liver-derived enzymes, aspartate aminotransferase (AST), or alanine aminotransferase (ALT), ruling out a nonspecific hepatitis; (b) in HFF mice, insulin signaling in muscle dramatically increased after administration of adenovirus encoding KI-PKC- $\zeta$ , corroborating that adenovirus did not substantially enter or produce untoward effects in muscle; (c) in HFF mice, aPKC activity was diminished in liver, but substantially increased in muscle following administration of adenovirus encoding KI-PKC- $\zeta$ , in keeping with exclusive functional localization of adenovirus in liver; (d) aPKC levels were increased in liver but not in muscle, further attesting to liver localization of adenovirus encoding KI-PKC- $\zeta$ ; (e) unlike hepatic aPKC activity, hepatic PKB/Akt activity was unchanged or, if anything, slightly increased above normal after administration of adenovirus encoding KI-PKC- $\zeta$ , indicating that insulin signaling to nonaPKC factors was not impaired; and (f) food intake was unaffected by adenoviral treatments. In attempts to analogously use adenovirus encoding KI-PKB, there were marked decreases in food intake and body weight, thus invalidating this approach. PKC- $\lambda$  and PKC- $\zeta$  can function interchangeably during insulin action, and KI forms of either isoform inhibit both aPKC isoforms.

### Measurement of SREBP-1c, FAS, ACC, IL-1 $\beta$ , and TNF $\alpha$ mRNA

As described (17), tissues were added to Trizol reagent (Invitrogen), and RNA was extracted and purified with the RNA-Easy Mini-Kit from Qiagen (Valencia, CA) and RNAase-free DNAase set (Qiagen) as per kit instructions, quantified by measuring A<sub>260</sub>/A<sub>280</sub>, further checked for purity by electrophoresis on 1.2% agarose gels, and mRNA quantified by quantitative real-time reverse transcriptase-polymerase chain reaction (RT-PCR). Reverse transcription was accomplished with TaqMan reverse transcription reagent from Applied Biosystems (Foster City, CA). SREBP-1c mRNA was measured with a SYBR Green kit (Applied Biosystems) using nucleotide primers ATCGGCGCGGAAGCTGTCGGGGTAGCGTC (forward) and ACTGTCTTGTTGATGAGCTGGAGCAT (reverse). Mouse fatty acid synthase mRNA (FAS) was measured with primers GAGGACACTCAAGTGGCTGA (forward) and GTGAGGTTGCTGTCTGTCTGT (reverse). Mouse acetyl CoA carboxylase (ACC) mRNA was measured with primers GACTTCATGAATTTGCTGAT (forward) and AAGCTGAAAGCTTTCTGTCT (reverse). Mouse interleukin-1 $\beta$  (IL-1 $\beta$ ) mRNA was measured with primers TTGGACGGACCCCAAAA-GATG (forward) and AGAAGGTGCTCATGTCTCTCA (reverse). Mouse tissue necrosis factor- $\alpha$  (TNF $\alpha$ ) mRNA was measured with primers ACGGCATGGATCTCAAAGAC (forward) and AGATAGCAAATCGGCTGACG (reverse). Mouse glucose-6-phosphatase (G6Pase) mRNA was measured with primers TGCTGCTCACTTCCCCACCAG (forward) and TCTCCAAAGTCCACAGGAGGT (reverse). Mouse phosphoenolpyruvate carboxylase (PEPCK) mRNA was measured with primers GACAGCCTGCCCCAGGCAGTGA (forward) and CTGGCCACATCTCGAGGGTCTAG (reverse). The housekeeping gene, hypoxanthine phosphoribosyltransferase (HPRT; used for recovery correction), was measured with primers TGAAAGACTTGCTCGAGATGTCA (forward) and AAAGAAGTATAGCCCCCCTTGA (reverse).

### Nuclear fraction preparation

As described (17), liver nuclei were prepared with NE-PER Nuclear and Cytoplasmic Extraction Reagents obtained from Pierce Biotechnology (Cat. No. 78833). Levels of the active SREBP-1 fragment and active p65/RelA subunit of NF $\kappa$ B were measured in these nuclear preparations, which were also used for electrophoretic mobility shift assays (EMSA).

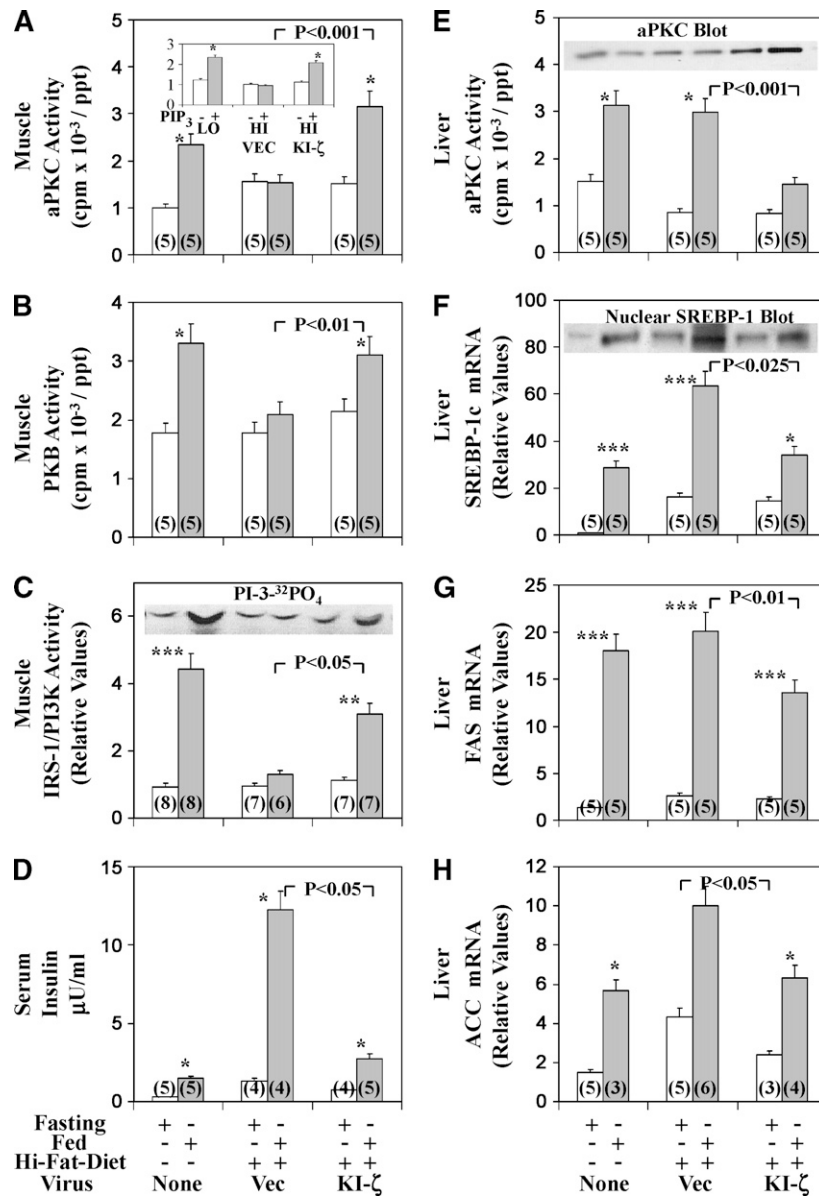


**Fig. 1.** Effects of adenoviral-mediated expression of kinase-inactive (KI) PKC- $\zeta$  on basal and feeding-induced activities of aPKC (A), PKB (B), and IRS-1-dependent PI3K (C) in vastus lateralis muscle, serum insulin levels (D), and basal and feeding-induced activity of aPKC (E), expression and nuclear levels of SREBP-1c (F), and expression of FAS (G) and ACC (H) in liver of high-fat-fed mice. High-fat-fed mice were injected IV with adenovirus vector (Vec) or adenovirus encoding KI-PKC- $\zeta$  (KI- $\zeta$ ) and 4 days later (to allow time for expression), mice were fasted overnight 16–20 h (clear bars) or maintained on the high-fat diet (shaded bars). For comparisons in assays, normal-chow-fed mice were similarly fasted or maintained on their usual normal chow (low-fat) diet. The mice were killed on the next day (fifth day after initial virus treatment), and muscles, livers, and sera were harvested. In the inset in panel A, aPKCs were immunoprecipitated from muscles of normal-chow-fed (LO) or high-fat-fed (HI) mice treated with adenovirus vector (VEC) or adenovirus encoding KI- $\zeta$ , and assayed in absence (clear bars) or presence (shaded bars) of 10  $\mu$ M PIP<sub>3</sub>. Values are mean  $\pm$  SEM of (N) determinations. Asterisks indicate  $P < 0.05$  (\*),  $P < 0.01$  (\*\*), and  $P < 0.001$  (\*\*\*) for feeding-stimulated values versus adjacent fasting values of mice fed a comparable high or normal (low fat) diet, or in the inset of panel A, PIP<sub>3</sub>-treated versus untreated. Portrayed  $P$  values depict comparisons of indicated groups (viz., insulin-stimulated adenovirus vector versus insulin-stimulated adenovirus encoding KI-PKC- $\zeta$  in high-fat-fed mice). All  $P$  values were determined by ANOVA. Insets show 10  $\mu$ M PIP<sub>3</sub>-dependent activation of aPKC immunoprecipitated from muscles of indicated mice (Panel A); representative autoradiograms of PI-3-<sup>32</sup>PO<sub>4</sub>, the lipid product of the PI3K assay (C); expressed KI-PKC- $\zeta$ -induced increases in levels of hepatic total aPKC (E); and a representative immunoblot of the active nuclear SREBP-1 fragment (F).

## Electrophoretic mobility shift assays

NF $\kappa$ B-dependent shifts in mobility of specific  $^{32}$ PO $_4$ -labeled DNA sequences was measured with a kit and NF $\kappa$ B consensus nucleotide probes (5'-AGTTGAGGGGACTTTCCCAGGC-3' and 3'TCAACTCCCCTGAAAGGGTCCG-5') obtained from Invitrogen [Cat. Nos. E3050 (kit) and E3291 (probe)].

## Serum insulin, triglyceride, free fatty acids, cholesterol, and glucose levels

Serum insulin, triglycerides, free (non-esterified) fatty acids (FFA), total cholesterol, HDL-cholesterol, and glucose levels were measured as described (17).

## Liver triglycerides

Liver triglycerides were measured as described (17).

## Statistical evaluations

Data are expressed as mean  $\pm$  SE, and *P* values were determined by a two-way ANOVA and the least-significant multiple comparison method.

## RESULTS

### HFF mice

*Insulin signaling in muscle and liver of HFF mice.* Impairments in insulin activation of aPKC and PKB/Akt previously observed in muscles of HFF mice (1, 2) were presently found to be associated with (a) markedly diminished activation of IRS-1– but not IRS-2–dependent PI3K (insulin activation data not shown, but see Fig. 1C for impaired effects of feeding and Fig. 2B for impaired insulin effects on aPKC activation); (b) poor responsiveness of aPKC immunoprecipitated from HFF muscle to direct addition of the lipid product of PI3K, PIP $_3$  (Fig. 1A inset and Fig. 2B) versus excellent response in aPKC immunoprecipitated from muscles of normal-chow–fed mice; and (c) marked impairment in insulin-stimulated glucose transport (Fig. 2A). This impairment in aPKC responsiveness to insulin and PIP $_3$  in HFF muscle was not explained by diminished phosphoinositide-dependent protein kinase-1 (PDK1)–dependent thr-411 phosphorylation, which was intact and in fact largely activated even “basally” in HFF mice (Fig. 2C), perhaps by endogenous hyperinsulinemia (Fig. 1D); rather, the impairment apparently reflected reduced PIP $_3$ –dependent auto-phosphorylation, allosteric modification, and/or aPKC catalytic activity that occurs subsequent to PDK-1 action (24–26).

In HFF liver, along with reported intactness of insulin effects on aPKC and PKB/Akt (1), the activation of both IRS-1– and IRS-2–dependent PI3K by insulin was indistinguishable from that seen in normal liver (not shown).

*Insulin-like signaling effects of feeding in muscle and liver of normal-chow-fed mice.* Relative to overnight-fasted mice, normal chow feeding was associated with higher activities of muscle aPKC (Fig. 1A), muscle PKB/Akt (Fig. 1B), muscle IRS-1–dependent PI3K (Fig. 1C), hepatic aPKC (Fig. 1E), hepatic PKB/Akt (see Ref. 6), and, moreover, hepatic SREBP-1c expression, as per mRNA and active nuclear

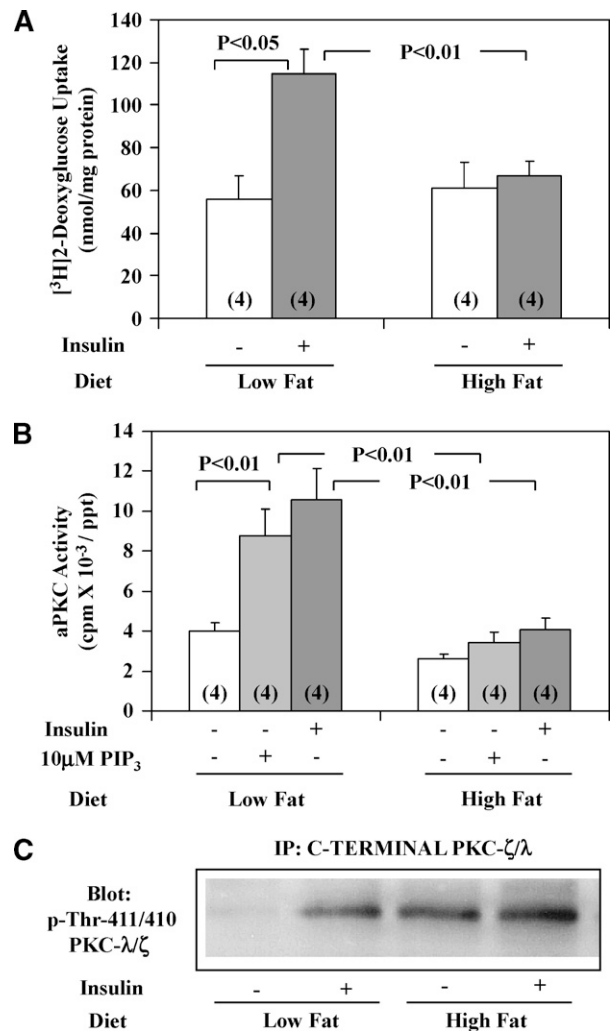


**Fig. 2.** Effects of insulin on [ $^3\text{H}$ ]2-deoxyglucose uptake (A), and effects of insulin and/or PIP $_3$  on aPKC activity (B) and phosphorylation of the activation loop site in aPKC (C) in vastus lateralis muscles of high-fat–fed (high fat) and chow-fed (low fat) mice. Mice were injected IP as described in Experimental Procedures (A). aPKCs were immunoprecipitated from muscles of mice treated IM with saline vehicle or insulin (1U/kg) in saline for 15 min, and then assayed in absence or presence of 10  $\mu\text{M}$  PIP $_3$  (B and C). It was necessary to first immunoprecipitate (IP) aPKC (because other 70–80 kDa PKCs have similar activation loop phosphorylation sites) before Western analyses for phospho-thr-411/410-PKC- $\lambda/\zeta$ ; shown here is a blot representative of four determinations (C). Values in panels A and B are mean  $\pm$  SE of (N) determinations. *P* values were determined by ANOVA.

fragment levels (Fig. 1F), and SREBP-1c–regulated expression of hepatic FAS (Fig. 1G) and ACC (Fig. 1H). These effects of feeding on signaling are qualitatively similar to those of insulin (1), but overnight fasting diminishes basal activities of insulin-sensitive signaling factors (viz., IRS-1/2–dependent PI3K, aPKC, and PKB/Akt in both muscle and liver), and feeding elicits submaximal but presumably physiological increases that can be further amplified by exogenous insulin treatment.

*Effects of insulin on IKK $\beta$ /NF $\kappa$ B and SREBP-1c in liver and muscle of normal-chow-fed mice.* As discussed above, IKK $\beta$  and NF $\kappa$ B are regulated by aPKC (7–10), but insulin effects are

unknown. We found that, like SREBP-1c, insulin treatment for 6 h activated IKK $\beta$  and NF $\kappa$ B (active nuclear levels of the p65/RelA/NF $\kappa$ B subunit and NF $\kappa$ B-dependent EMSA gel-shift activity) in livers of normal-chow-fed mice (Fig. 3). Different from liver, in muscle, 6-h insulin treatment failed to increase IKK $\beta$  and NF $\kappa$ B activation despite increasing expression and activity of SREBP-1c (Fig. 3).

*Dependence of feeding-dependent increases in hepatic activities of IKK $\beta$ /NF $\kappa$ B and SREBP-1c on aPKC in normal-chow-fed mice.* It was previously reported that partial depletion of hepatic aPKC by liver-specific knockout of PKC- $\lambda$  in mice is accompanied by diminished normal-chow-feeding-induced SREBP-1c activation, and enhanced glucose tolerance and

insulin sensitivity, relative to wild-type mice (4). Presently, we found that, using Cre-loxP methods (i.e., administration of adenovirus expressing Cre-recombinase to mice with floxed PKC- $\lambda$  genes) (17) provoked a partial but substantial loss of aPKC selectively in liver (muscle aPKC levels were unaffected), and this was accompanied by marked inhibition of feeding-induced increases in activities of not only hepatic SREBP-1c but also of IKK $\beta$ /NF $\kappa$ B in normal-chow-fed mice (Fig. 4). With respect to the residual hepatic immunoreactive hepatic aPKC (Panel A) after treatment with adenovirus encoding Cre-recombinase to selectively deplete hepatic PKC- $\lambda$ , mouse liver contains substantial amounts of PKC- $\zeta$  mRNA and protein (see Ref. 17 and presently confirmed).

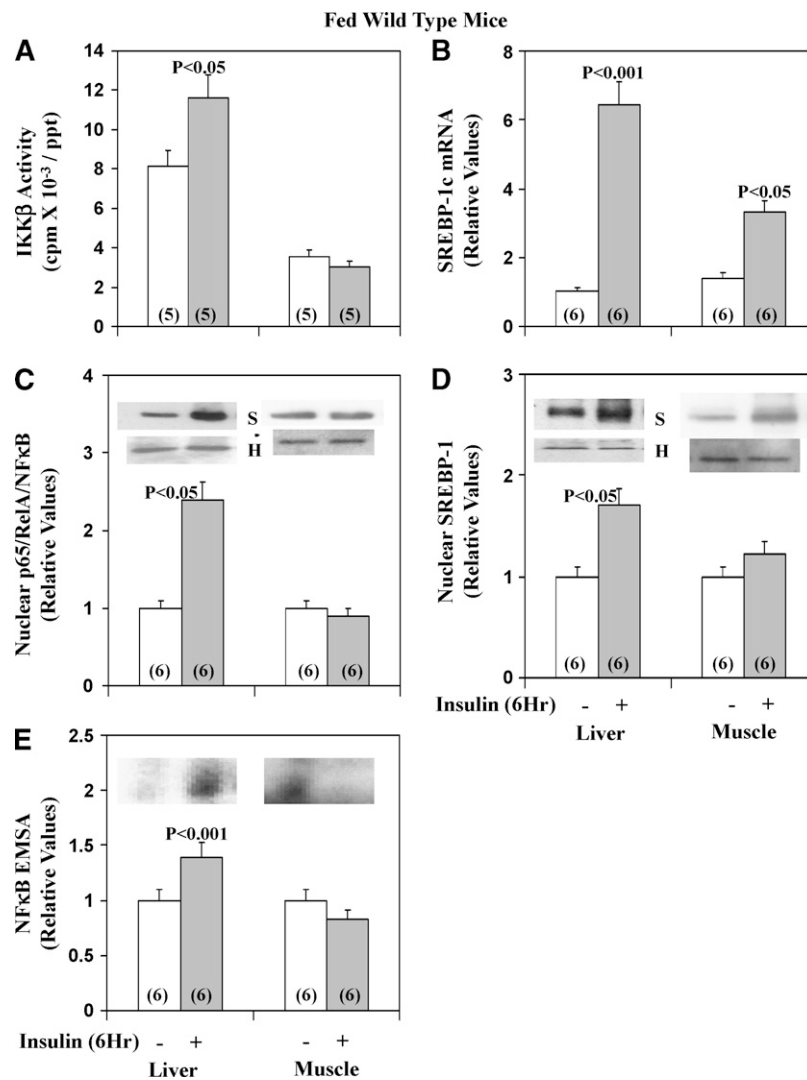


**Fig. 3.** Effects of insulin on IKK $\beta$  activity (A), nuclear NF $\kappa$ B p65/RelA/NF $\kappa$ B levels (C), NF $\kappa$ B electrophoretic mobility shift assay (EMSA) activity (E), SREBP-1c mRNA (B), and active nuclear SREBP-1 fragment levels (D) in liver and skeletal muscle. Long-acting glargine insulin (60mU/gm body wt) or physiological saline was administered subcutaneously to normal-chow-fed mice at approximately 8 AM, 6 h before killing and harvesting of liver and muscle. Values are mean  $\pm$  SEM of (N) determinations. P-values (as per ANOVA) depict comparisons of indicated groups (viz., insulin-stimulated versus saline-treated control mice). In bar graphs, values were normalized to unity for each tissue and do not reflect marked differences in immunoreactivity between tissues. Immunoblots are shown for histone (H) loading controls (note lack of significant differences between samples), as well as for NF $\kappa$ B (N) and SREBP-1 (S).

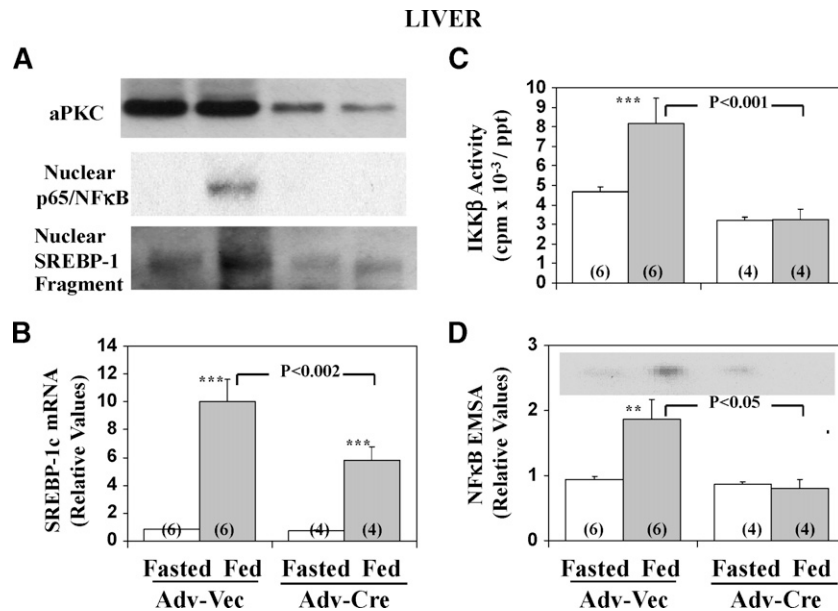


**Fig. 4.** Effect of depletion of hepatic PKC- $\lambda$  on feeding-dependent increases in hepatic nuclear levels of immunoreactive p65/RelA/NF $\kappa$ B and the active SREBP-1 fragment (A), SREBP-1c mRNA (B), IKK $\beta$  activity (C) and NF $\kappa$ B electrophoretic mobility shift assay (EMSA) activity (D). Mice with two floxed PKC- $\lambda$  alleles (17) were treated IV with adenovirus (Adv-Vec) or adenovirus encoding Cre-recombinase (Adv-Cre). Four weeks later, the mice were fasted overnight or allowed their usual normal-chow diet (fed), and then killed. Values are mean  $\pm$  SEM of (N) determinations. Asterisks indicate  $P < 0.05$  (\*),  $P < 0.01$  (\*\*), and  $P < 0.001$  (\*\*\*) for feeding-stimulated values (shaded bars) versus adjacent basal fasting values (clear bars).  $P$  values (as per ANOVA) depict comparisons of indicated groups (viz., feeding-stimulated adenoviral-Cre-treated mice versus feeding-stimulated adenoviral-vector-treated mice). Panel A also shows levels of hepatic total aPKC [mouse liver contains comparable amounts of PKC- $\lambda$  and PKC- $\zeta$  mRNAs (Ref. 4 and confirmed in our lab)]; this explains the residual aPKC seen after Cre-recombinase-mediated loss of PKC- $\lambda$ . Representative autoradiogram of the electrophoretically purified NF $\kappa$ B-DNA complex seen in the EMSA (D). See Fig. 5 for further description of EMSA autoradiographic findings.

*Effects of feeding in muscle and liver of HFF mice.* Relative to normal-chow-fed mice, in HFF mice, feeding-dependent increases in activities of aPKC (Fig. 1A), PKB/Akt (Fig. 1B), and IRS-1-dependent PI3K (Fig. 1C) were markedly diminished in muscle; however, in liver, as with insulin stimulation (1), feeding-dependent increases in aPKC activity (Fig. 1E) and PKB/Akt activation/phosphorylation were unaltered (see Ref. 1 and note in Fig. 7 intact feeding-dependent activation of PKB/Akt-dependent G6Pase and PEPCK genes). Thus, even with physiological dietary-induced increases in insulin secretion, aPKC and PKB/Akt activation was largely conserved in HFF liver.

In keeping with conserved hepatic aPKC activation and the presence of insulin resistance and hyperinsulinemia (Fig. 1D) in HFF mice, fasting and feeding-dependent increases in hepatic SREBP-1c mRNA (Fig. 1F), SREBP-1c active nuclear fragment levels (Fig. 1F), and ACC mRNA (Fig. 1H) were inordinately increased, relative to chow-fed mice. On the other hand, FAS mRNA was similarly increased in fed HFF and normal-chow-fed mice (Fig. 1G), perhaps reflecting maximal activation.

In livers of HFF mice, there were marked increases in activity of IKK $\beta$ , active nuclear levels of p65/RelA/NF $\kappa$ B subunit, and nuclear NF $\kappa$ B-dependent EMSA gel-shift activity; in contrast to 6-h insulin treatment, NF $\kappa$ B activity was not altered by acute 15-min insulin treatment (Fig. 5B).

*Effects of KI-PKC- $\zeta$  on hepatic aPKC, PKB, SREBP-1c, FAS, ACC, and triglycerides.* Following administration of adenovirus encoding KI-PKC- $\zeta$  to HFF mice, whereas total hepatic aPKC immunoreactivity increased (Fig. 1E inset), HFF-dependent increases in hepatic aPKC activity were markedly reduced (Fig. 1E bar graph); in contrast, increases in hepatic PKB/Akt activation were unchanged (not shown). Importantly, the reduction in hepatic aPKC activation in HFF mice was accompanied in liver by decreases in HFF-dependent increases in SREBP-1c mRNA and active nuclear fragment levels (Fig. 1F) and expression of SREBP-1c-regulated genes [viz., FAS (Fig. 1G) and ACC (Fig. 1H) mRNA]; moreover, hepatic triglyceride content diminished to levels comparable to those of chow-fed mice (Fig. 6A).

*Effects of KI-PKC- $\zeta$  on hepatic NF $\kappa$ B activation.* As with SREBP-1c activation, treatment of HFF mice with adenovirus encoding KI-PKC- $\zeta$  markedly diminished the inordinate HFF-dependent increases in IKK $\beta$  (Fig. 5A) and NF $\kappa$ B activities (Fig. 5B) [total cellular hepatic p65/RelA/NF $\kappa$ B levels were not altered before or after KI-PKC- $\zeta$  treatment (not shown)]. In addition, there were decreases in mRNA levels of hepatic cytokines, IL1- $\beta$ , and TNF $\alpha$  (Fig. 6A), genes regulated by NF $\kappa$ B.

*Effects of KI-PKC- $\zeta$  on insulin signaling in muscle.* Remarkably, in HFF mice the impairments in feeding-dependent

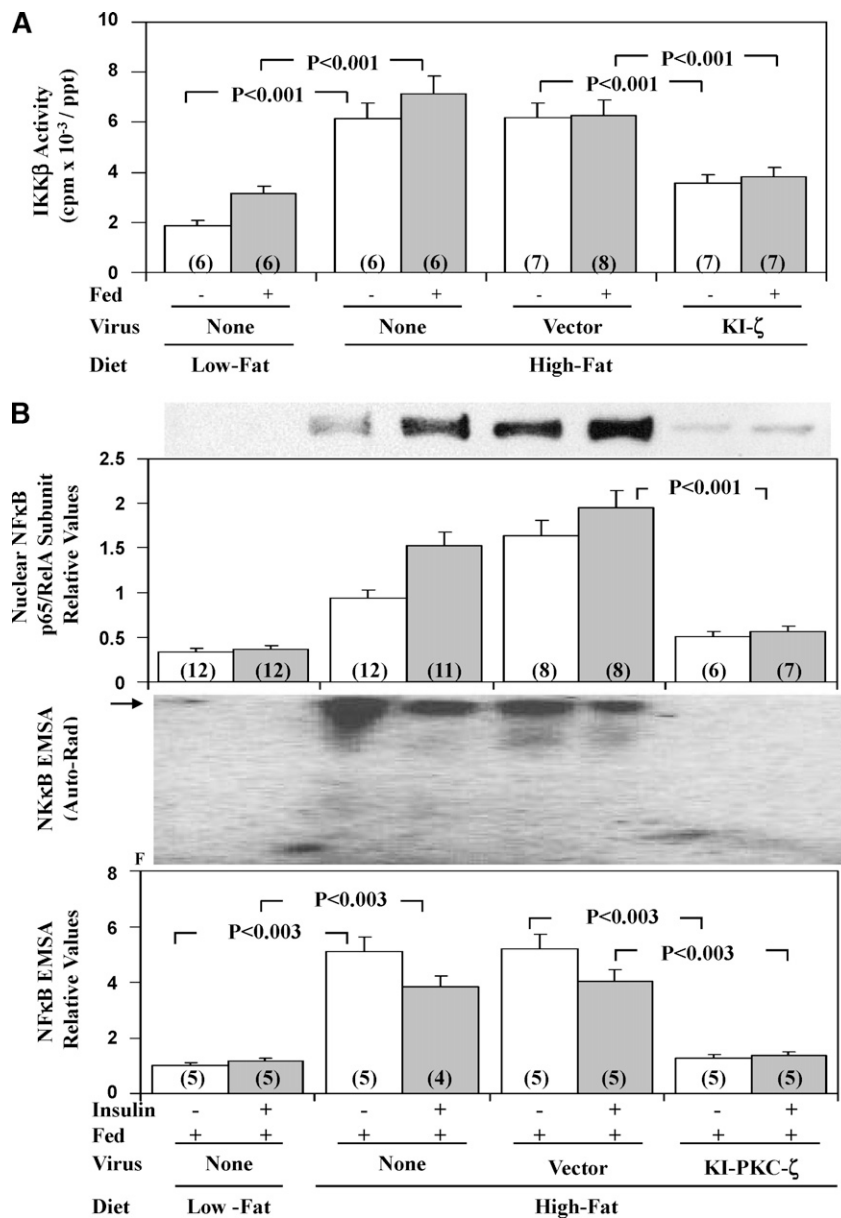


**Fig. 5.** Effects of adenoviral-mediated expression of kinase-inactive PKC- $\zeta$  on hepatic IKK $\beta$  activity (A), hepatic nuclear levels of the p65/RelA subunit of NF $\kappa$ B (B), and NF $\kappa$ B-dependent EMSA mobility shifts (B), in high-fat-fed (HFF) mice. As in Fig. 1, where indicated, HFF mice were injected IV with adenovirus vector (Vec) or adenovirus encoding KI-PKC- $\zeta$  (KI- $\zeta$ ), and 5 days later (to allow time for expression), mice were either fasted overnight or fed, or fed and treated IM for 15 min with saline or insulin in saline. For comparisons in assays, chow-fed (low fat) mice were similarly examined. Values are mean  $\pm$  SEM of (N) determinations and *P* values (as per ANOVA) depict comparisons of indicated groups. Representative immunoblot of nuclear levels of the p65/RelA subunit of NF $\kappa$ B, and a representative autoradiogram of NF $\kappa$ B-dependent EMSA mobility shifts (arrow indicates electrophoretic mobility of the NF $\kappa$ B-DNA complex as determined with the kit standard (B)). F indicates the electrophoretic front, as well as relative changes in multiple samples in the indicated groups.

activation of IRS-1-dependent PI3K (Fig. 1C), aPKC (Fig. 1A), PKB/Akt (Fig. 1B), and the defect in aPKC responsiveness to PIP<sub>3</sub> (Fig. 1A inset) in muscle were largely reversed to or toward normal after treatment with adenovirus encoding KI-PKC- $\zeta$ . Levels of aPKC, IRS-1, and PKB/Akt in HFF muscle were unaltered (not shown).

*Effects of KI-PKC- $\zeta$  on serum insulin levels.* Feeding provoked increases in serum insulin levels (Fig. 1D), and such

increases were inordinate in HFF mice. Moreover, administration of adenovirus encoding KI-PKC- $\zeta$  markedly diminished serum insulin levels of fed HFF mice virtually to normal. This improvement in serum insulin presumably at least partly reflected improved insulin action in muscle.

*Effects of KI-PKC- $\zeta$ -mediated inhibition of hepatic aPKC on serum triglyceride, cholesterol, and glucose levels.* Along with inordinate increases in HFF-dependent activation of hepatic



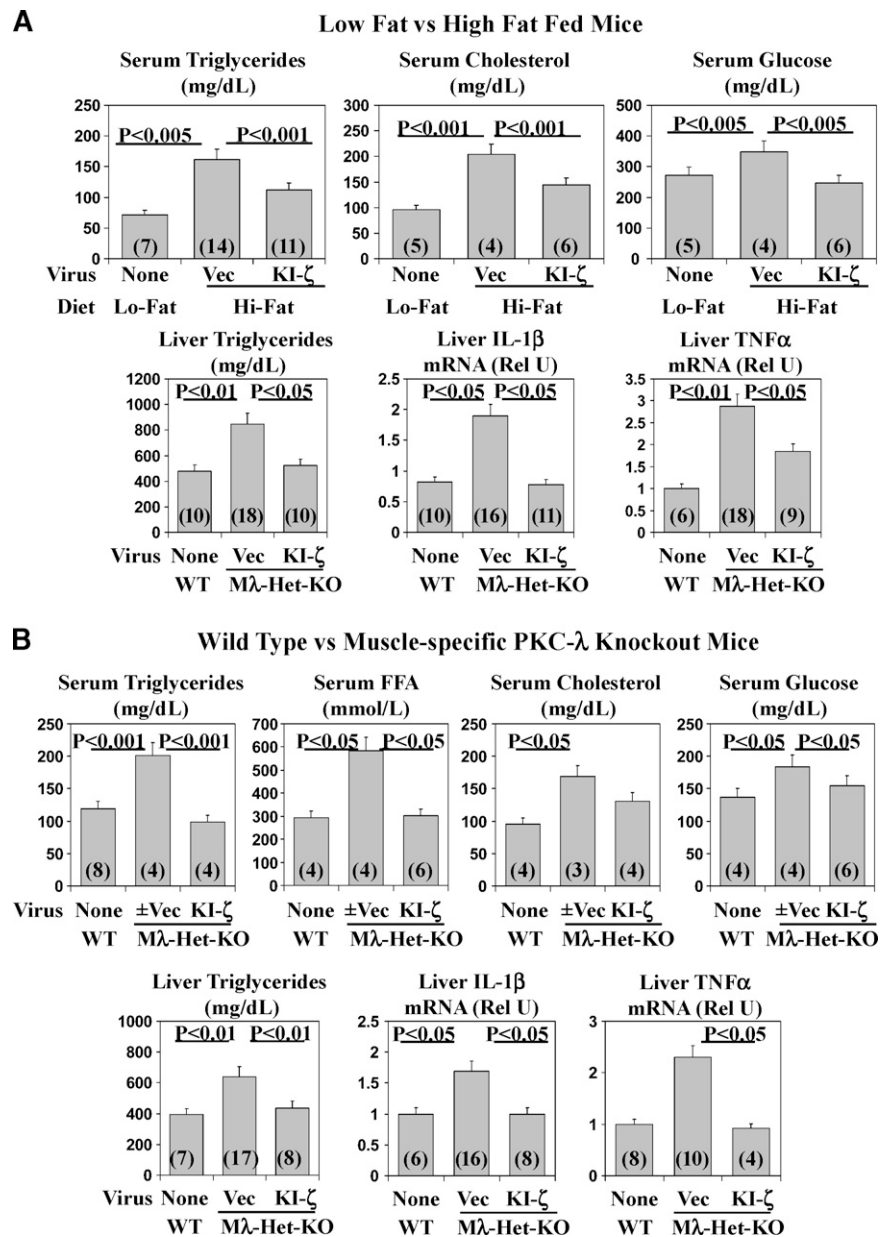


**Fig. 6.** Effects of administration of adenovirus encoding kinase-inactive PKC- $\zeta$  (KI- $\zeta$ ) on fasting serum levels of triglycerides, free fatty acids (FFA), total cholesterol, and glucose; and hepatic levels of triglycerides, ACC mRNA, IL-1 $\beta$  mRNA, and TNF $\alpha$  mRNA in high-fat-fed mice (A) and heterozygous muscle-specific PKC- $\lambda$  knockout (M $\lambda$ -Het-KO) mice (B). WT = wild-type mice. Vec = adenovirus vector. Rel U = relative units. Values are mean  $\pm$  SEM of (N) determinations and *P* values (as per ANOVA) depict comparisons of indicated groups.

SREBP-1c, the serum levels of triglycerides, total cholesterol, and glucose were elevated above those seen in normal-chow-fed mice and, more interestingly, diminished substantially toward normal after 5 days of treatment with adenovirus encoding KI-PKC- $\zeta$  (Fig. 6A).

*Effects of KI-PKC- $\zeta$ -mediated inhibition of hepatic aPKC on hepatic G6Pase and PEPCK expression.* Like insulin, feeding in normal-chow-fed mice provoked decreases in expression of hepatic enzymes important in gluconeogenesis and glucose release [viz., as per PEPCK and G6Pase mRNA levels (Fig. 7)]. In HFF mice, fasting levels of these mRNAs

trended downward, perhaps reflecting inhibitory effects of hyperinsulinemia, and feeding elicited further decreases in these mRNAs (Fig. 7). Interestingly, administration of adenovirus encoding KI-PKC- $\zeta$ , if anything, caused a further downward trend (albeit statistically insignificant) in fasting levels of these mRNAs. (However, note statistically significant decreases in fasted G6Pase and PEPCK mRNA levels elicited by adenovirus encoding KI-PKC- $\zeta$  in studies of M $\lambda$ -Het-KO mice described below.) Most importantly, mRNA levels of G6Pase and PEPCK in fed mice were comparably low, regardless of either dietary fat content (i.e., high fat versus low fat) or treatment with adenovirus

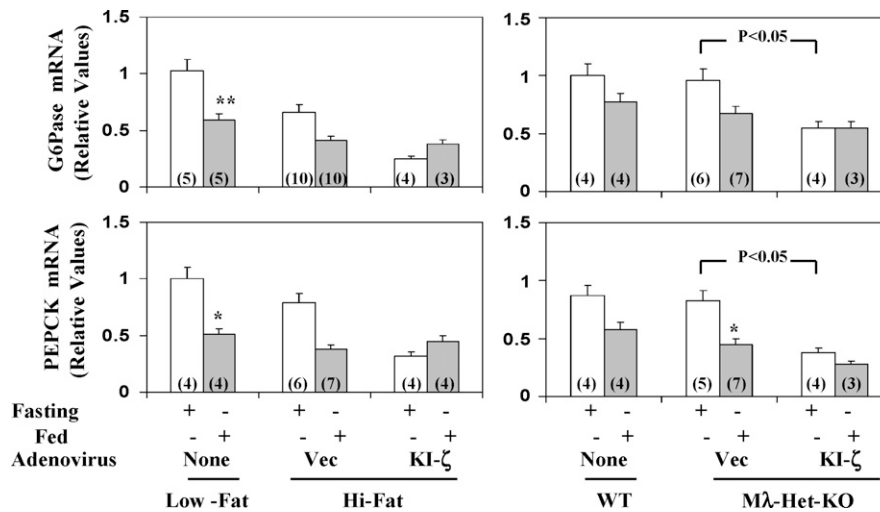


**Fig. 7.** Effects of administration of adenovirus encoding kinase-inactive PKC- $\zeta$  (KI- $\zeta$ ) on fasting and fed levels of hepatic G6Pase mRNA and PEPCK mRNA in high-fat-fed mice (left) and heterozygous muscle-specific PKC- $\lambda$  knockout (M $\lambda$ -Het-KO) mice (right). For comparisons in assays, samples from control mice on normal mouse chow (low fat) and wild-type (WT) littermates of M $\lambda$ -Het-KO mice were employed. Vec = adenovirus vector. Values are mean  $\pm$  SEM of (N) determinations. Asterisks indicate  $P < 0.05$  (\*) and  $P < 0.01$  (\*\*) for feeding-stimulated values (shaded bars) versus adjacent fasting values (clear bars).  $P$  values depict comparisons of indicated groups. All  $P$  values were determined by ANOVA.

encoding KI-PKC- $\zeta$ . These findings suggested that feeding/insulin regulation of these genes in both presently studied obesity models was essentially intact and, moreover, in concert with the idea that feeding/insulin-induced decreases in expression of G6Pase and PEPCK genes are independent of aPKC and instead largely depend on PKB/Akt. In fact, as further discussed below in studies of M $\lambda$ -Het-KO mice, as administration of adenovirus encoding KI-PKC- $\zeta$  clearly diminished G6Pase and PEPCK mRNA levels in fasting mice, it is possible that aPKC contributes to the maintenance of higher levels of these mRNAs in fasting conditions; such maintenance would most likely be independent of but reversible by insulin treatment.

#### M $\lambda$ -Het-KO mice

In M $\lambda$ -Het-KO mice, we reported that muscle aPKC levels are diminished, insulin activation of residual muscle aPKC activation is impaired, and insulin-stimulated glucose transport in muscle is diminished. On the other hand, normal-chow-feeding-dependent hepatic SREBP-1c and FAS activation is inordinately increased, and insulin activation of PKB/Akt in both muscle and liver is intact or, if anything, enhanced (17). Moreover, M $\lambda$ -Het-KO mice have hyperinsulinemia, mild hyperglycemia, hyperlipidemia, and hepatosteatosis (17). Presently, as in HFF mice, administration of adenovirus encoding KI-PKC- $\zeta$  to M $\lambda$ -Het-KO mice elicited decreases in feeding-dependent activation of hepatic aPKC (Fig. 8A), and this was attended by decreases in (a) hepatic levels of SREBP-1c mRNA (Fig. 8B), active nuclear SREBP-1c fragment (Fig. 8C), and ACC mRNA (Fig. 8D); (b) activities of hepatic IKK $\beta$  (Fig. 8E) and NF $\kappa$ B, as per EMSA gel-shift activity (Fig. 8F) and levels of the active nuclear p65/RelA/NF $\kappa$ B subunit (Fig. 8G); and (c) mRNA levels of NF $\kappa$ B-regulated cytokines, IL-1 $\beta$

(Fig. 6B) and TNF $\alpha$  (Fig. 6B). Hepatic triglyceride levels, and serum levels of triglycerides, free fatty acids, and glucose, all of which are elevated in M $\lambda$ -Het-KO mice (17), were similarly elevated in adenovirus vector-treated M $\lambda$ -Het-KO mice and, more importantly, diminished to levels seen in wild-type mice, along with similar downward trends in serum cholesterol levels following administration of adenovirus encoding KI-PKC- $\zeta$  and inhibition of hepatic aPKC (Fig. 6B). As in HFF studies, hepatic levels of G6Pase and PEPCK mRNA were comparably low in fed wild-type and M $\lambda$ -Het-KO mice, regardless of treatment administration of the latter group with adenovirus encoding KI-PKC- $\zeta$  (Fig. 7). On the other hand, as discussed above, the fasting levels of these mRNAs were significantly diminished by treatment with adenovirus encoding KI-PKC- $\zeta$  in M $\lambda$ -Het-KO mice, perhaps suggesting that aPKC contributes to maintaining expression of G6Pase and PEPCK genes in the fasting state (also note similar downward trends of these mRNAs with adenoviral/KI- $\zeta$  treatment in high-fat studies).

#### DISCUSSION

In livers of both obesity models, HFF and M $\lambda$ -Het-KO mice, the expression of SREBP-1c and levels of its active nuclear fragment were, as expected, inordinately elevated but, even more importantly, diminished markedly following inhibition of hepatic aPKC activity by adenovirally mediated expression of KI-PKC- $\zeta$ . It therefore seems clear that aPKC played a critical role in feeding/insulin-dependent increases in hepatic SREBP-1c expression in both obesity models. Moreover, it was important to see in both obesity models that decreases in activation of hepatic aPKC and expression of SREBP-1c, within 5 days of treatment with

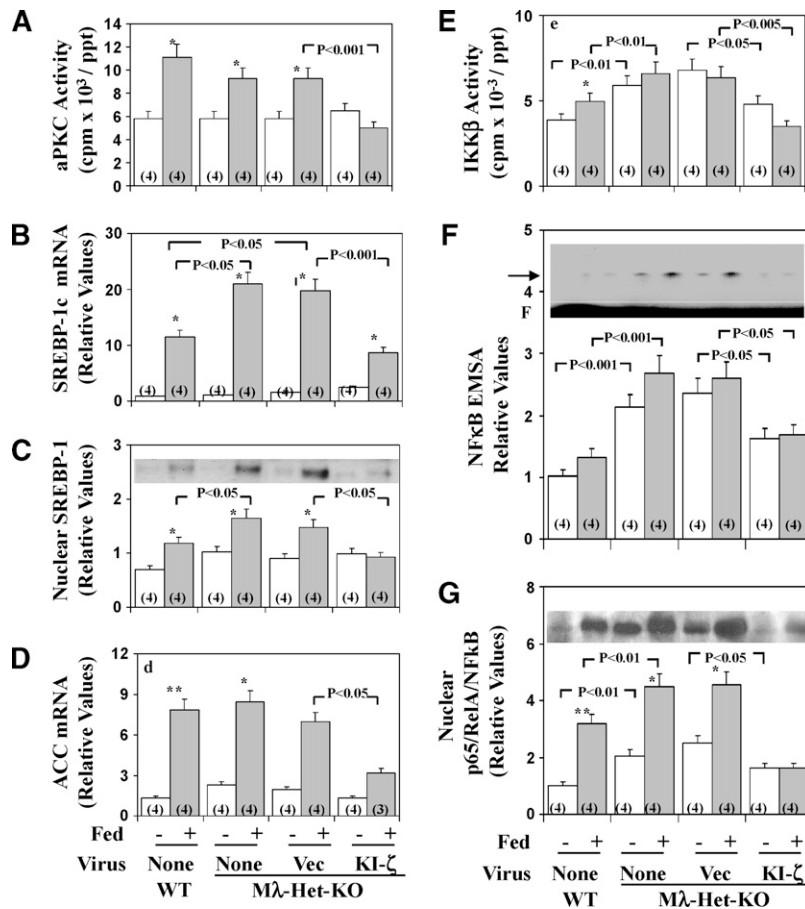


**Fig. 8.** Effects of adenovirally mediated expression of kinase-inactive (KI) PKC- $\zeta$  on basal and feeding-induced hepatic aPKC activity (A), SREBP-1c mRNA (B), active nuclear SREBP-1 fragment (C), ACC mRNA (D); IKK $\beta$  activity (E), NF $\kappa$ B electrophoretic mobility shift assay (EMSA) activity (F), and nuclear p65/RelA/NF $\kappa$ B subunit levels (G) in heterozygous muscle-specific PKC- $\lambda$  knockout (M $\lambda$ -Het-KO) mice. M $\lambda$ -Het-KO mice were either not injected (None) or injected IV with adenovirus vector (Vec) or adenovirus encoding KI-PKC- $\zeta$  (KI- $\zeta$ ). Four days later (to allow time for expression), mice were fasted overnight (clear bars) or maintained on their usual low-fat, normal-chow diet (shaded bars). For comparisons in assays, wild-type (WT) littermates were similarly fasted or maintained on low-fat, normal-chow diet. Mice were killed on the fifth day after virus treatment, and muscles, livers, and sera were harvested. Values are mean  $\pm$  SEM of (N) determinations. Arrow in panel F indicates electrophoretic mobility of the NF $\kappa$ B-DNA complex as determined with the kit standard; F indicates the electrophoretic front. Asterisks indicate  $P < 0.05$  (\*),  $P < 0.01$  (\*\*), and  $P < 0.001$  (\*\*\*) for feeding-stimulated values versus adjacent basal fasting values.  $P$  values depict comparisons of indicated groups. All  $P$  values were determined by ANOVA. Representative immunoblots of the active nuclear SREBP-1 fragment and the nuclear p65/RelA/NF $\kappa$ B subunit (C and G insets, respectively). Representative autoradiogram of an NF $\kappa$ B EMSA gel-shift assay (F inset).

adenovirus encoding KI-PKC- $\zeta$ , were attended by (a) substantial decreases in hepatic mRNA levels of SREBP-1c-regulated genes, FAS and ACC, and (b) marked improvements (virtually to normal) in hepatic triglyceride levels and serum levels of triglycerides, free fatty acids, total cholesterol, insulin, and glucose. Thus, it is clear that hepatic aPKC plays a crucial role in hepatic lipid synthesis and the pathogenesis of hepatosteatosis and hyperlipidemia in these murine obesity models.

Perhaps equally important were findings in both obesity models showing that hepatic IKK $\beta$  and NF $\kappa$ B activities and genes of NF $\kappa$ B-regulated cytokines, IL-1 $\beta$  and TNF $\alpha$ , which collectively have been linked to the development of systemic insulin resistance in HFF mice (7, 8), were inordinately increased. Again, treatment with adenovirus en-

coding KI-PKC- $\zeta$  diminished hepatic IKK $\beta$  and NF $\kappa$ B activities and IL-1 $\beta$  and TNF $\alpha$  mRNA levels. In this regard, it was important to find in normal-chow-fed mice that (a) insulin treatment over 6 h provoked increases in hepatic IKK $\beta$  and NF $\kappa$ B activities and (b) liver-specific knockout of PKC- $\lambda$  (following administration of adenovirus encoding Cre-recombinase to PKC- $\lambda$ -floxed mice) markedly diminished feeding effects on hepatic IKK $\beta$  and NF $\kappa$ B. Thus, it appears that both insulin and feeding (perhaps via endogenous insulin, at least in part) activate hepatic IKK $\beta$ /NF $\kappa$ B as well as hepatic SREBP-1c, and both activations are to a great extent dependent on hepatic aPKC.

Notably, in HFF mice, within 5 days of adenoviral treatment with KI-PKC- $\zeta$  and subsequent decreases in hepatic SREBP-1c and IKK $\beta$ /NF $\kappa$ B activities, there were remarkable

improvements in insulin signaling to IRS-1–dependent PI3K, aPKC, and PKB/Akt in skeletal muscle. Moreover, hyperinsulinemia in HFF mice was largely reversed by this treatment with adenovirus encoding KI-PKC- $\zeta$ , presumably reflecting, at least partly, the improvement of insulin action in muscle. On the other hand, in M $\lambda$ -Het-KO mice, other than for impaired aPKC activation owing to the irreversible depletion of PKC- $\lambda$ , there are no impairments in insulin signaling in muscle (17), thus precluding our ability to observe alterations (i. e., improvements) in insulin signaling in muscle following inhibition of hepatic aPKC.


Of further interest, ancillary findings in presently used HFF mice that insulin effects on IRS-1–dependent PI3K (but not IRS-2-dependent PI3K) were impaired in muscle, and insulin effects on both IRS-1– and IRS-2–dependent PI3K were intact in liver suggested that (a) impaired activation of IRS-1–dependent PI3K accounted for impaired insulin signaling to aPKC and PKB/Akt in muscle and (b) intact activation of both IRS-1– and IRS-2–dependent PI3K in liver accounted for conserved activation of hepatic PKB/Akt (and subsequent regulation of G6Pase, PEPCK, and SREBP-1c genes) and hepatic aPKC in HFF mice. Our findings further suggested that, in addition to impaired IRS-1–dependent PI3K activation, impaired responsiveness of aPKC to PIP<sub>3</sub> contributed to diminished aPKC activation in HFF muscle.

From the present findings, it may be reasoned that persistent hyperinsulinemia in obesity and other insulin-resistant states contributes importantly to increases seen in hepatic IKK $\beta$  and NF $\kappa$ B activities through the activation of hepatic aPKC. However, other aPKC activators (e.g., cytokines and lipids) may also contribute to increases in aPKC, IKK $\beta$ , and NF $\kappa$ B activities in liver and other tissues in these insulin-resistant states. In either case, inhibition of IKK $\beta$  by high-dose salicylate therapy improves insulin action in muscle and liver in insulin-resistant rodents (7, 8), presumably by diminishing NF $\kappa$ B-dependent circulating inflammatory cytokines, such as IL-6 (7, 8) and TNF- $\alpha$ . Accordingly, it is likely that improvements in insulin signaling in muscle presently observed in HFF mice after treatment with adenoviruses that inhibit hepatic aPKC at least partly reflect diminished hepatic IKK $\beta$ /NF $\kappa$ B activation by insulin and possibly other agonists.

Although we were able to significantly diminish expression of hepatic lipid-synthesizing enzymes and both hepatic and serum lipid levels, there were only modest statistically insignificant decreases in actual liver size during the 5-day period of treatment of HFF mice with adenovirus encoding KI-PKC- $\zeta$ . Nevertheless, there was remarkable improvement in serum insulin levels and the ability of insulin to activate IRS-1–dependent PI3K, aPKC, and PKB/Akt in muscles of HFF mice following adenoviral/ KI-PKC- $\zeta$  treatment. Whether improvements in insulin signaling in muscle were caused by decreases in hepatic lipid synthesis and diminished serum lipid levels, or diminished hepatic NF $\kappa$ B activation, or both, is uncertain.

From the present findings, it may be surmised that chronic activation of hepatic aPKC in hyperinsulinemic states is associated with undesirable consequences of (a) excessive

synthesis of hepatic enzymes that promote lipid synthesis and thereby enhance tendencies to obesity, hepato-steatosis, and hyperlipidemia, and (b) excessive activation of hepatic inflammatory factors that impair systemic insulin sensitivity and glucose tolerance and promote thrombotic tendencies in atherosclerotic processes. On the other hand, the activation of muscle aPKC is critically needed for insulin stimulation of Glut4 glucose transporter translocation and glucose transport in muscle (17), and an isolated defect in aPKC action in muscle leads to glucose intolerance, hyperinsulinemia, abdominal obesity, hepatosteatosis, and hyperlipidemia, as reported previously (17) and corroborated in the presently used M $\lambda$ -Het-KO model. From the present results, it is reasonable to propose that hyperinsulinemia resulting from muscle-specific knockout of aPKC and subsequent the impairment in glucose transport in muscle provokes inordinate increases in hepatic lipid synthesis and hyperlipidemia and, perhaps over time, abdominal obesity in this experimental model. Accordingly, it may be surmised that, in muscle, aPKC serves as an anti-diabetes/anti-obesity factor, whereas, in liver, when chronically activated, as in obesity and type 2 diabetes, aPKC serves as a pro-diabetes/pro-obesity factor. In this regard, it is important to note that, despite observations of aPKC deficiency in muscles of type 2 diabetic humans (23, 27), in initial studies, we have not observed a deficiency of aPKC in livers of type 2 diabetics (unpublished observations – U. Varanasi, M.P. Sajan, S. Nimal, R.V. Farese).

Finally, our findings suggest that a therapeutic agent that selectively inhibits the activation of hepatic aPKC but spares muscle aPKC activation would be particularly efficacious for treating insulin-resistant states of obesity and type 2 diabetes. Development of such an agent will be a challenging but potentially rewarding endeavor. 

## REFERENCES

1. Standaert, M. L., M. P. Sajan, A. Miura, Y. Kanoh, H. C. Chen, R. V. Farese, Jr., and R. V. Farese. 2004. Insulin-induced activation of atypical protein kinase C, but not protein kinase B, is maintained in diabetic *ob/ob* and Goto-Kakizaki liver. Contrasting insulin signaling patterns in liver versus muscle define phenotypes of type 2 diabetic and high fat-induced insulin-resistant states. *J. Biol. Chem.* **279**: 24929–24934.
2. Chen, H. C., R. Rao, M. P. Sajan, M. L. Standaert, Y. Kanoh, A. Miura, R. V. Farese, Jr., and R. V. Farese. 2004. Role of adipocyte-derived factors in enhancing insulin signaling in skeletal muscle and white adipose tissue of mice lacking acyl CoA:diacylglycerol transferase 1. *Diabetes*. **53**: 1445–1451.
3. Taniguchi, C. M., T. Kondo, M. P. Sajan, J. Luo, R. Bronson, T. Asano, R. V. Farese, L. C. Cantley, and C. R. Kahn. 2006. Divergent regulation of hepatic glucose and lipid metabolism by phosphoinositide 3-kinase via Akt and PKC-lambda/zeta. *Cell Metab.* **3**: 343–353.
4. Matsumoto, M., W. Ogawa, K. Akimoto, H. Inoue, K. Miyaki, K. Furukawa, Y. Hayashi, H. Iguchi, Y. Marsuki, R. Hiramatsu, et al. 2003. PKC $\lambda$  in liver mediates insulin-induced SREBP-1c expression and determines both hepatic lipid content and overall insulin sensitivity. *J. Clin. Invest.* **112**: 935–944.
5. Fleischmann, M., and P. B. Iynedjian. 2000. Regulation of sterol regulatory-element binding protein expression in liver: role of insulin and protein kinase B/Akt. *Biochem. J.* **349**: 13–17.
6. Zhang, W., S. Patil, B. Chauhan, S. Guo, D. R. Powell, J. Le, A. Klotsas, R. Matika, X. Xiao, R. Franks, et al. 2006. FoxO1 regulates multiple metabolic pathways in the liver: effects on gluconeogenic, glycolytic and lipogenic gene expression. *J. Biol. Chem.* **281**: 10105–10117.

7. Cai, D., M. Yuan, D. F. Frantz, P. A. Melendez, L. Hansen, J. Lee, and S. E. Shoelson. 2005. Local and systemic insulin resistance resulting from hepatic activation of IKK-beta and NF-kappaB. *Nat. Med.* **11**: 183–190.
8. Shoelson, S. E., L. Herrero, and A. Naaz. 2007. Obesity, inflammation and insulin resistance. *Gastroenterology*. **132**: 2169–2180.
9. Lallena, M.-J., M. T. Diaz-Meco, G. Bren, C. V. Pay, and J. Moscat. 1999. Activation of I $\kappa$ B kinase $\beta$  by protein kinase C isoforms. *Mol. Cell. Biol.* **19**: 2180–2188.
10. Duran, A., M. T. Diaz-Meco, and J. Moscat. 2003. Essential role of RelA Ser311 phosphorylation by  $\zeta$ PKC in NF- $\kappa$ B transcriptional activation. *EMBO J.* **22**: 3910–3918.
11. Anai, M., M. Funaki, A. Ogiwara, Y. Onishi, H. Sakoda, K. Inukai, M. Nawano, Y. Fukushima, Y. Yazaki, M. Yazaki, Y. Oka, and T. Asano. 1999. Enhanced insulin-stimulated activation of phosphatidylinositol 3-kinase in the liver of high-fat-fed rats. *Diabetes*. **48**: 158–169.
12. Kanoh, Y., M. P. Sajan, G. Bandyopadhyay, A. Miura, M. L. Standaert, and R. V. Farese. 2003. Defective activation of atypical protein kinase C  $\zeta$  and  $\lambda$  by insulin and phosphatidylinositol-3,4,5- $PO_4$  in skeletal muscle of rats following high-fat feeding and streptozotocin-induced diabetes. *Endocrinology*. **144**: 947–954.
13. Tremblay, F., C. Lavigne, H. Jacques, and A. Marette. 2001. Defective insulin-induced GLUT4 translocation in skeletal muscle of high fat-fed rats is associated with alterations of both Akt/protein kinase B and atypical protein kinase C  $\zeta/\lambda$  activities. *Diabetes*. **50**: 1901–1910.
14. Ueki, K., T. Yamauchi, H. Tamemoto, K. Tobe, R. Yamamoto-Honda, Y. Akanuma, Y. Kaburagi, Y. Yazaki, S. Aizawa, R. Nagai, et al. 2000. Restored insulin-sensitivity in IRS-1-deficient mice treated by adenovirus-mediated gene therapy. *J. Clin. Invest.* **105**: 1437–1445.
15. Sajan, M. P., M. L. Standaert, A. Miura, and R. V. Farese. 2004. Tissue-specific differences in activation of atypical protein kinase C and protein kinase B in muscle, liver and adipocytes of insulin receptor substrate-1 knockout mice. *Mol. Endocrinol.* **18**: 2513–2521.
16. Valverde, A. M., D. J. Burks, I. Fabregat, T. L. Fisher, J. Carretero, M. F. White, and M. K. Benito. 2003. Molecular mechanisms of insulin resistance in IRS-2-deficient hepatocytes. *Diabetes*. **52**: 2239–2248.
17. Farese, R. V., M. P. Sajan, H. Yang, P. Li, S. Mastorides, W. J. Gower, Jr., S. Nimal, C. S. Choi, S. Kim, G. I. Shulman, et al. 2007. Muscle-specific knockout of protein kinase C- $\lambda$  impairs glucose transport and induces metabolic and diabetic syndromes. *J. Clin. Invest.* **117**: 2289–2301.
18. Kanoh, Y., G. Bandyopadhyay, M. P. Sajan, M. L. Standaert, and R. V. Farese. 2001. Rosiglitazone, insulin treatment and fasting correct defective activation of protein kinase C- $\zeta/\lambda$  by insulin in vastus lateralis muscles and adipocytes of diabetic rats. *Endocrinology*. **142**: 1595–1605.
19. Leitges, M., M. Plomann, M. L. Standaert, G. Bandyopadhyay, M. P. Sajan, Y. Kanoh, and R. V. Farese. 2002. Knockout of PKC $\alpha$  enhances insulin signaling through PI3K. *Mol. Endocrinol.* **16**: 847–858.
20. Standaert, M. L., G. Bandyopadhyay, L. Galloway, J. Soto, Y. Ono, U. Kikkawa, R. V. Farese, and M. Leitges. 1999. Effects of knockout of the protein kinase C  $\beta$  gene on glucose transport and glucose homeostasis. *Endocrinology*. **140**: 4470–4477.
21. Yu, B., M. L. Standaert, T. Arnold, H. Hernandez, J. Watson, K. Ways, D. R. Cooper, and R. V. Farese. 1992. Effects of insulin on diacylglycerol/protein kinase-C signalling and glucose transport in rat skeletal muscle *in vivo* and *in vitro*. *Endocrinology*. **130**: 3345–3355.
22. Bandyopadhyay, G., Y. Kanoh, M. P. Sajan, M. L. Standaert, and R. V. Farese. 2000. Effects of adenoviral gene transfer of wild-type, constitutively active, and kinase-defective protein kinase C- $\lambda$  on insulin-stimulated glucose transport in L6 myotubes. *Endocrinology*. **141**: 4120–4127.
23. Beeson, M., M. P. Sajan, M. Dizon, D. Grebnev, J. Gomez-Daspert, A. Miura, Y. Kanoh, J. Powe, G. Bandyopadhyay, M. L. Standaert, et al. 2003. Activation of protein kinase C- $\zeta$  by insulin and phosphatidylinositol-3,4,5-( $PO_4$ ) $_3$  is defective in muscle in type 2 diabetes and impaired glucose intolerance: amelioration by rosiglitazone and exercise. *Diabetes*. **52**: 1926–1934.
24. Standaert, M. L., G. Bandyopadhyay, Y. Kanoh, M. P. Sajan, and R. V. Farese. 2001. Insulin and PIP $_3$  activate PKC- $\zeta$  by mechanisms that are both dependent and independent of phosphorylation of activation loop T410 and autophosphorylation T560 sites. *Biochemistry*. **40**: 249–255.
25. Le Good, J. A., W. H. Ziegler, D. B. Parekh, D. R. Alessi, P. Cohen, and P. J. Parker. 1998. Protein kinase C isotopes controlled by phosphoinositides-3-kinase through protein kinase PDK1. *Science*. **281**: 2042–2045.
26. Chou, M. M., W. Hou, J. Johnson, L. K. Graham, M. Lee, H. Chen, A. C. Newton, B. S. Schaufhausen, and A. Toker. 1998. Regulation of protein kinase C $\zeta$  by PI 3-kinase and PDK-1. *Curr. Biol.* **8**: 1069–1077.
27. Kim, Y.B., K. Kotani, T. P. Ciaraldi, R. R. Henry, and B. B. Kahn. 2003. Insulin-stimulated protein kinase C- $\lambda/\zeta$  activity is reduced in skeletal muscle of humans with obesity and type 2 diabetes; reversal with weight reduction. *Diabetes*. **52**: 1935–1942.